Molecular Structures of ZnO by Aggregates of Atoms and Interaction of Two Monolayers

Cristian E. García-López, Irineo-Pedro Z. Rivera, Benjamín Vargas-Arista, and Verónica Estrella-Suarez

***Abstract*—The first-principles calculations are useful for determining electronic and structural properties for a model that simulates a material composed of atomic clusters of ZnO through the analysis of interaction energies and charge distribution. The two-dimensional structural form of ZnO aggregates shows regularly flat hexagons obtained in models of 6, 27 and 54 atoms of Zinc and Oxygen. The structure of a three-dimensional system was determined by dynamics calculations by using the interaction of a pair of monolayers consisting of 108 atoms and as a result, a cage structure was formed from a cluster of Zn54 and O54 identifying only bond atoms at the ends that promote the union of monolayers. The stable structure shows modifications of the atomic bonds in whose centers hexagonal rings prevailed and at the arrangements of the end of triangles, squares, pentagons and even rings of 10 and 11 atoms were obtained. Atomic positions and charge distribution were analyzed based on the methodology used Density Functional Theory (DFT), with the becke88-LYP exchange and correlation functional.**

***Index Terms*—Cluster ZnO, DFT, Molecular Dynamics, Nanostructures.**

I. Introduction

The electronic properties as well as the behavior of atoms in molecules are studied by calculations of first principles. These calculations make it possible to know the electronic structure of a molecular system made up of a set of functions that depend on the atomic and spin positions [1]. Zinc oxide is a semiconductor of interest in the technological field for its applications [2,3,4]. During the last decades an increase in applications was observed due to the extensive study and development of research to obtain useful properties in technological development with important contributions [5,6]. This material is currently considered a semiconductor synthesized through a process of new techniques, where growth brings new physical properties, as well as technological applications [7-10]. Zinc oxide has different electronegativities of zinc and oxygen, and the most stable crystalline structure is the hexagonal wurzite type [11-14]. Zinc oxide has technological interest and especially in nanometer-level structures, because it is possible to obtain nanostructures in the form of nanoparticles, where different structures are observed in both form and type, generating various nanostructures in the form of nanoparticles, nanowires, nanofiber, as the main ones. This makes zinc oxide acquire great interest for the various nanosystems such as optoelectronic devices, biosensors, pigment for the production of paints, and in the pharmaceutical industry such as the field of cosmetics used as an ultraviolet radiation filter in products such as creams solar. In the electronic aspect they are also used as acoustic transducers, varistors, gas sensors, transparent electrodes and optical window for solar cells. [15-19].

In this report, structural properties were determined from atomic aggregates through geometry optimization calculations. The first results show that aggregates with hexagonal structure formation prevail. From a two-dimensional system, the three-dimensional structure was generated. The development of molecular dynamics calculation was useful in the model of two interacting monolayers to obtain a stable structure. From the analysis of the structural results and the charge distribution, it was determined that various atomic arrangements occur in the peripheral zone of the monolayers where atomic clusters are identified for the ZnO, as a first approximation, structural forms resulting from the interaction between the two monolayers of hexagonal structure.

II. Methodology

In the theory of density functionalities where exchange energy is used in an atomic system, the behavior is asymptotic as an approximation to determine how the exchange energy affects density in addition to the corrected gradient presenting an asymptotic limit. appropriate under a single parameter that allows us to calculate the exact exchange energy implemented in the functional Becke 88 [20]. Lee-Yang-Parr (LYP) is another useful approximation for calculating correlation energy, which is expressed in terms of electronic density when considering a second-order operator to obtain the equation that calculates part of the density, as well as density of local kinetic energy expressed with expansions in the gradient, where the functional has elements to calculate energy and correlation potential [21]. The previous functionalities form a hybrid functional that constitutes the Becke88-LYP exchange and correlation

Published on October 30, 2019.

C. E. García-López is with the Tecnológico Nacional de México, Campus Instituto Tecnológico de Tlalnepantla Av. Instituto Tecnológico s/n, Col: La Comunidad, Tlalnepantla de Baz, Estado de México, C.P.: 54070 Apartado Postal 750 México (e-mail: author@ boulder.nist.gov).

I. P. Zaragoza is with the Tecnológico Nacional de México, Campus Instituto Tecnológico de Tlalnepantla Av. Instituto Tecnológico s/n, Col: La Comunidad, Tlalnepantla de Baz, Estado de México, C.P.: 54070 Apartado Postal 750 México (izaragoza@ittla.edu.mx).

B. Vargas-Arista is with the Tecnológico Nacional de México, Campus Instituto Tecnológico de Tlalnepantla Av. Instituto Tecnológico s/n, Col: La Comunidad, Tlalnepantla de Baz, Estado de México, C.P.: 54070 Apartado Postal 750 México (e-mail: author@nrim.go.jp).

V. Estrella-Suarez is with the Tecnológico Nacional de México, Campus Instituto Tecnológico de Tlalnepantla Av. Instituto Tecnológico s/n, Col: La Comunidad, Tlalnepantla de Baz, Estado de México, C.P.: 54070 Apartado Postal 750 México (e-mail: author@nrim.go.jp).

functional, being useful for the calculation of geometry optimization. In generals, the functional hybrids are considered as an approximation to obtain stable atomic structures, which allow to describe molecular electronic characteristics attached to experimental results from the level of DFT theory by including electronic correlation and spin-orbital corrections, in the non-local density approximation (NLDA). The non-local results favor the calculation of the electronic properties and the interaction energy for the molecules, presenting that the non-local is a better approximation in some molecular cases since it adequately explains the anisotropy for charge distribution attached to experimental values. The results of the geometry optimization calculations under this approximation scheme are used for molecules containing O and Zn atoms. The calculations involve all electrons in the DZVP basis set, considering neutral charge for the total system and multiplicity 1 to find baseline state. The electronic wave function is constructed from the approach when electrons are submerged in a field of static nuclei and the nuclei are considered as in a medium electronic field. Dynamics calculations are useful for knowing the favorable reaction mechanisms and for the formation of new molecular structures.

III. Results and Discussions

A. *Two-dimensional ZnO.*

The structure of a first model was formed by 3 atoms of oxygen and 3 of zinc, atoms continue to be added in equal proportion to observe the two-dimensional shape of a molecular structure of 24 atoms, the number of atoms is increased again to obtain a molecular system with 54 atoms, as seen in Fig. 1. Optimization calculations were performed to determine a stable structure where it is observed that a priority direction is followed in regular arrangements prevailing exchanges between the oxygen atom and zinc atom favoring the flat hexagon type for the three models.

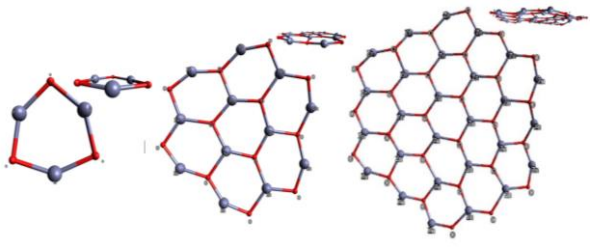

(a) (b) (c)

Fig. 1. The structural arrangements of ZnO atoms; a) model 6, b) model with 24 and c) model 54, the arrangements form rings similar to hexagons between the Zinc and Oxygen bonds with two-dimensional monolayers

In this stage, a relevant aspect is covered when determining the preferred direction from the structural point of view with stability associated with a minimum of energy by geometry optimization calculation results, as in the case shown in Fig. 1 c), with atoms of Zn_{27} and O_{27}.

B. *Molecular dynamics of the interaction between two monolayers of ZnO.*

The above structures are used to form a three-dimensional structure taking into account the interaction of atoms by calculating DFT dynamics. The model of the molecule is selected from 2 molecular structures like the one shown in Fig. 1 c). The procedure consists in leaving a fixed molecule and the other giving it a speed with separation distance relatively considering that the initial position indicates a zero interaction of the monolayers The dynamic calculation as a result of the interaction when placed in parallel shows that the collision is totally repulsive moving the monolayers away, in the first result of the calculation developed giving the energy value of -2728839.1 eV, as shown in Fig. 2.

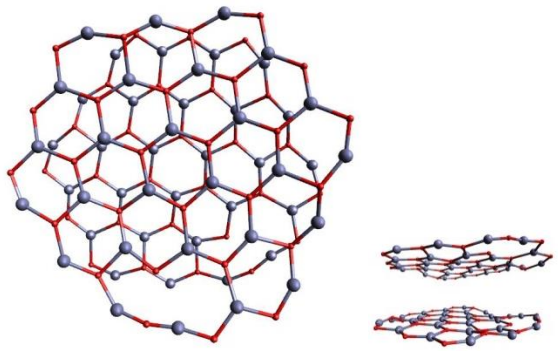

Fig. 2. Initial structure of the Zn_{54} O_{54} for the interaction of the two monolayers seen from the front and side when they interact in parallel.

The previous results propose to modify the initial position of the monolayers to carry out the interaction and obtain the three-dimensional structure. A monolayer was rotated so that the zinc atoms of a monolayer during the interaction are in the oxygen direction of the other monolayer to perform the dynamic calculation and consider this as the initial structure. For the interaction between monolayers, the energy values were obtained for each moment of time as reported in Fig. 3.

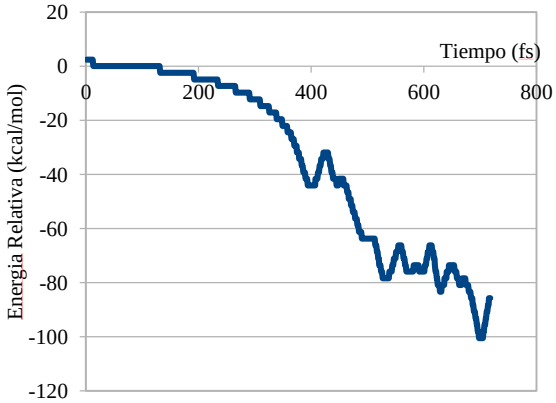

Fig. 3. The relative energy of the interaction as a function of time for the two monolayers shows a decrease in energy and is negative with the first minimum near the 400 fs persisting several minimums and maximums

The energy values obtained as a result of the dynamics are decreasing indicating that these values are associated with a different attraction interaction compared to the repulsive interaction obtained when they interacted in parallel. The values decrease to a minimum of -40 kcal/mol, instants later in 400 fs increase to a maximum of 10 kcal/mol, and then descend from -30 to -80 kcal/mol, comparing the structures at each instant of time it is observed that the maximums are associated to the reactions where a bond length modification for the extreme atoms of each monolayer is carried out.

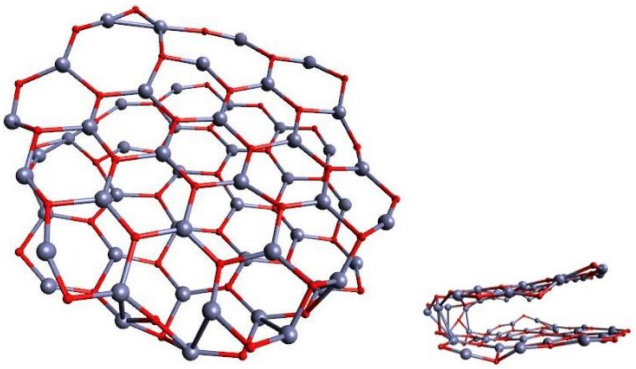

Fig. 4. Final structure of the interaction between the 2 monolayers through dynamics in two views, lateral and frontal.

The structure resulting from the interaction of the two monolayers starting from the initial structure by dynamic calculation gives a value of -2728839.1 eV taking into account the same conditions of the parallel interaction, observing that there is an interaction that promotes a sandwich structure appreciating bond atoms at the ends determining that the central atoms of the two monolayers have minimal modifications preserving the representative hexagons whose energy value -2728846.2 eV, obtaining a value whose difference is -7 eV due to structural changes, as shown in Fig. 4.

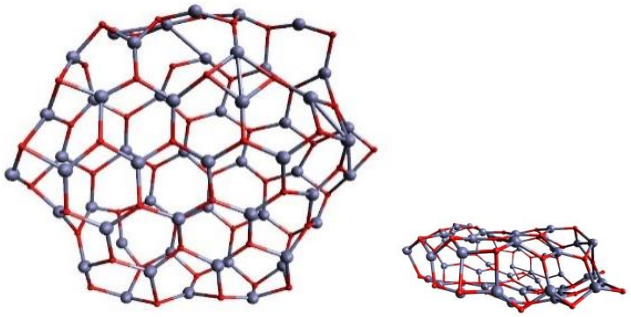

Fig. 5. The final stable molecular structure obtained from the sandwich structure as a ZnO aggregate of two monolayers, front and side view.

To determine the final structure by geometry optimization calculation for the two monolayers is made from the structure obtained by dynamics calculation is shaped like a sandwich, mentioning that the two monolayers do not change their flat shape. The result shows a final structure observing different types arising from one side of the dynamic interaction and the last calculation a stable structure as a three-dimensional molecule, where a small separation between centers of the monolayers is preserved describing a cage-like structure as shown in Fig. 5. Besides, different bonds for the Zn atoms represented by the larger atom and O represented by the smaller atom such as triangles Zn_2 O_1, squares Zn_2 O_2, pentagons Zn_3 O_2 were characterized in the figure of the final structure, and hexagons Zn_3 O_3. It is also observed that said interaction of the stable structure modifies the flat shape of the center of the monolayers.

C. Structural analysis and charge distribution for various structural forms of the ZnO.

The results of the interaction of the monolayers show different aggregates of O_{54} and Zn_{54} atoms, as shown in Fig. 5, where different atomic arrangements are observed at the ends. Atomic aggregates for the various forms of zinc oxide structure are analyzed to determine if there is an attachment to experimental results. The structures that form aggregates of atoms of hexagonal arrangements are according to the most stable hexagonal crystalline structure type wurtzite.

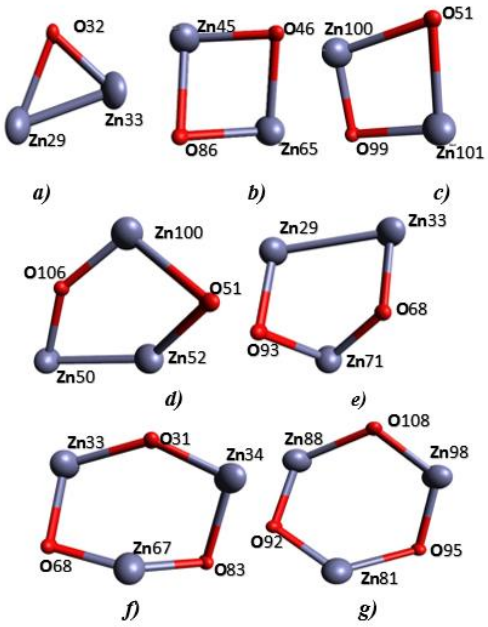

Fig. 6. a) 3 atoms show a triangular figure; b) and c) 4 atoms form a square of two types; d) and e) 5 atoms make up the pentagonal type structure coexisting two different; f) and g) 6 atoms show two pentagonal structures with atoms of large Zn and O represented by the smaller atom.

TABLE I: MULLIKEN POPULATION ANALYSIS, LENGTH AND ANGLE FOR FIG. 6

Mulliken population analysis		Distance		Angle *(°)*		
Atom	Charge	Bond	Length *(Å)*	Angle *(°)*	Initial Atom - Vertex Atom Final Atom	
Zn_{29}	29.19	Zn_{29}-O_{32}	1.93425	46.502	O_{32}- Zn_{29} –Zn_{33}	a
Zn_{33}	29.21	Zn_{33}-O_{32}	1.88735	45.057	O_{32}-Zn_{33}-Zn_{29}	
O_{32}	8.74	O_{32}-Zn_{33}	1.88735	88.440	Zn_{29}- O_{32} – Zn_{33}	
Zn_{65}	29.24	Zn_{65}-O_{86}	2.0045	90.662	O_{86}-Zn_{65}-O_{46}	B
O_{86}	8.73	Zn_{65}-O_{86}	2.0045	85.900	Zn_{65}-O_{86}-Zn_{45}	
Zn_{45}	29.24	O_{46}-Zn_{45}	1.98176	92.040	O_{86}-Zn_{45}-O_{46}	
O_{46}	8.73	O_{46}-Zn_{65}	2.16522	85.767	Zn_{65}-O_{46}-Zn_{45}	
Zn_{100}	29.18	Zn_{100}-O_{99}	2.20622	96.247	O_{99}-Zn_{100}-Zn_{101}	C
O_{99}	8.74	O_{99}-Zn_{51}	1.94478	76.944	Zn_{100}-O_{99}-Zn_{101}	
Zn_{101}	29.14	Zn_{101}-O_{99}	2.18838	99.942	O_{99}-Zn_{101}-O_{51}	
O_{51}	8.88	O_{51}-Zn_{100}	2.04707	86.416	Zn_{100}-O_{51}-Zn_{101}	
Zn_{50}	29.18	Zn_{50}-Zn_{52}	2.66547	64.840	O_{106}-Zn_{50}-Zn_{52}	D
Zn_{52}	29.08	Zn_{52}-O_{51}	1.97855	132.19	O_{51}-Zn_{52}-Zn_{50}	
Zn_{100}	29.18	$Zn_{100}O_{106}$	2.07685	102.07	O_{51}-Zn_{100}-O_{106}	
O_{106}	8.88	O_{106}-Zn_{50}	1.91335	144.58	Zn_{50}-O_{106}-Zn_{100}	
O_{51}	8.86	O_{51}-Zn_{50}	2.16493	86.793	Zn_{52}-O_{51}-Zn_{100}	
Zn_{29}	29.19	Zn_{71}-O_{93}	1.94265	102.14	Zn_{33}-Zn_{29}-O_{93}	E
Zn_{33}	29.21	Zn_{71}-O_{68}	1.91142	73.983	Zn_{29}-Zn_{33}-O_{68}	
Zn_{71}	29.19	O_{93}-Zn_{29}	1.95881	126.62	Zn_{33}-O_{29}-Zn_{71}	
O_{68}	8.76	O_{68}-Zn_{33}	1.920	88.307	O_{68}-Zn_{71}-O93	
O_{93}	8.72	Zn_{29}-Zn_{33}	2.79495	99.367	Zn_{29}-O_{93}-Zn_{71}	
Zn_{81}	29.07	Zn_{81}-O_{92}	1.93221	121.07	O_{95}-Zn_{81}-O_{92}	F
Zn_{88}	29.08	Zn_{88} -O_{108}	1.85653	121.50	O_{92}-Zn_{88}-O_{108}	
Zn_{98}	29.13	Zn_{98}-O_{92}	2.00285	121.27	O_{108}-Zn_{98}-O_{95}	
O_{92}	8.93	O_{92}-Zn_{88}	1.97982	110.74	Zn_{88}-O_{92}-Zn_{81}	
O_{95}	8.93	O_{95}-Zn_{98}	2.10278	111.90	Zn_{81}-O_{95}-Zn_{98}	
O_{108}	8.95	O_{108}-Zn_{98}	1.95058	116.17	Zn_{88}-O_{108}-Zn_{98}	
Zn_{33}	29.21	Zn_{33}-O_{83}	1.90936	109.75	O_{68}-Zn_{33}-O_{31}	G
Zn_{34}	29.21	Zn_{34}-O_{31}	1.9425	103.00	O_{31}-Zn_{34}-O_{83}	
Zn_{67}	29.22	Zn_{67}-O_{68}	1.88919	148.75	O_{68}-Zn_{67}-O_{83}	
O_{31}	8.83	O_{31} -Zn_{33}	2.09444	139.90	Zn_{33}-O_{31}-Zn_{34}	
O_{68}	8.76	O_{68}-Zn_{33}	1.92	95.961	Zn_{33}-O_{68}-Zn_{67}	
O_{83}	8.76	O_{83}-Zn_{34}	2.03761	97.827	Zn_{67}-O_{83}-Zn_{34}	

The structure of our three-dimensional model shows a region of monolayers where they prevail with hexagonal arrangements mainly in the center but in contrast at the ends where there are no regular arrangements with existing atomic bonds with a triangular, square shape, until they reach structures with ten atoms attached. The bonds that appear in the first instance describe three atom bonds as seen in Fig. 6, identifying that an oxygen atom bonded to two zinc atoms prevails. In the next structure 4 bonds, two types that correspond to 2 oxygen and 2 zinc with different prevail, what varies are the angles which modify the separation distance between the two zinc atoms, identifying two different forms. In the case of 5 bonds, there are 2 oxygen and 3 zinc but having an excess of zinc there is a tendency of bonding between two zinc. Also, there is the case of 6 bonds in an equitable way, there are 3 oxygen and 3 zinc, with the sequence of one oxygen and one zinc, observing that the length of the bonds varies along with the angles that form between the atoms prevailing the hexagon. The values in Table I shows the charge distribution, the bond length with the neighboring atom and the angle with the nearby neighbors where the oxygen with excess and the zinc with deficiency in the charge distribution reflected its effects on the length of the atomic bond as well as the angle between the different atoms. The irregular shapes of the final structure of Fig. 7 show that there is a further set of asymmetric figures formed by atoms of Zn as the largest atom and O the smallest atom that forms structures of seven bonds between Zn_4 and O_3, eight bonds between Zn_4 and Zn_4 O_4 and ten bond between Zn_5 and O_5

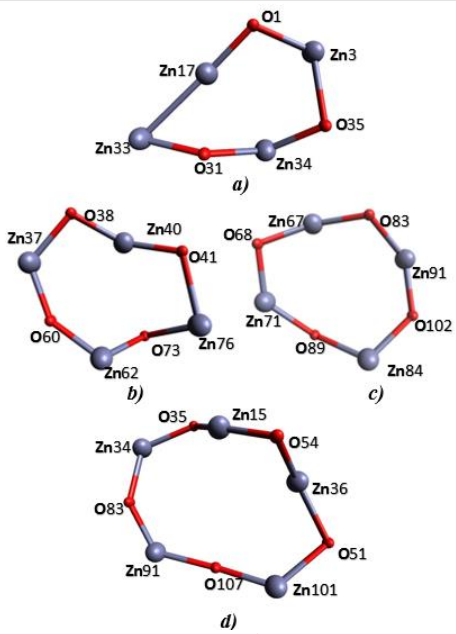

Fig. 7. a) 7 atoms without a regular figure; b) and c) 8 atoms form an equivalent form without regular structure with two types; d) 10 atoms make up another structure without regularity for the atoms of Zn of large size and O atom of smaller size

Table II shows mainly by the bonds of atoms and angles that there is no regularly well-defined structure, so it is considered an irregular structure, detecting the variation between the angles of zinc-oxygen-zinc bond prevailing varied values in the angles for the structures of Fig. 7. In the case of ZnO structures that form pairs, Zn is well defined, followed by consecutive O. However, what is relevant in Fig. 7 and Table I is when the union between zinc and zinc only happens when the number of atoms is odd.

TABLE II: MULLIKEN POPULATION ANALYSIS, LENGTH AND ANGLE FOR FIG. 7

Mulliken population analysis		Distance		Angle *(°)*		
Átom	Charge	Bond	Length *(Å)*	Angle *(°)*	Initial Atom - Vertex Atom Final Atom .	
O_1	8.96	O_1-Zn_{17}	1.96288	111.82	Zn_3-O_1-Zn_{17}	A
O_{31}	8.801	O_{31}-Zn_{34}	1.9425	139.90	Zn_{33}-O_{31}-Zn_{34}	
O_{35}	8.77	O_{35}-Zn_3	2.24714	105.13	Zn_3-O_{35}-Zn_{34}	
Z_{n3}	29.15	Zn_3-O_1	2.01407	110.55	O_1-Zn_3-O_{35}	
Zn_{17}	29.17	Zn_{17}-Zn_{33}	2.77179	170.45	O_1-Zn_{17}-Zn_{33}	
Zn_{33}	29.21	Zn_{33}-Zn_{17}	2.77179	55.226	Zn_{17}-Zn_{33}-O_{31}	
Zn_{34}	29.21	Zn_{34}-O_{35}	1.9817	124.98	O_{31}-Zn_{34}-O_{35}	
O_{73}	8.7	O_{73}-Zn_{37}	1.98674	102.76	Zn_{37}-O_{73}-Zn_{40}	B
O_{60}	8.71	O_{60}-Zn_{76}	2.24821	113.96	Zn_{40}-O_{60}-Zn_{76}	
O_{41}	8.73	O_{41}-Zn_{37}	1.89433	143.32	Zn_{37}-O_{41}-Zn_{62}	
O_{38}	8.92	O_{38}-Zn_{76}	1.98925	102.26	Zn_{62}-O_{38}-Zn_{76}	
Zn_{37}	29.16	Zn_{37}-O_{73}	1.98674	93.918	O_{60}-Zn_{37}-O_{38}	
Zn_{40}	29.22	Zn_{40}-O_{60}	1.84622	148.95	O_{73}-Zn_{40}-O_{60}	
Zn_{62}	29.2	Zn_{62}-O_{38}	1.92349	113.69	O_{41}-Zn_{62}-O_{38}	
Zn_{76}	29.24	Zn_{76}-O_{73}	1.88696	120.35	O_{73}-Zn_{76}-O_{41}	
O_{68}	8.76	O_{68}-Zn_{67}	1.88919	120.56	Zn_{67}-O_{68}-Zn_{71}	C
O_{83}	8.76	O_{83} -Zn_{67}	1.90936	105.43	Zn_{67}-O_{83}-Zn_{91}	
O_{89}	8.93	O_{89}-Zn_{71}	1.87607	126.17	Zn_{71}-O_{89}-Zn_{84}	
O_{102}	8.93	O_{102}-Zn_{91}	2.04536	132.66	Zn_{84}-O_{102}-Zn_{91}	
Zn_{67}	29.22	Zn_{67}-O_{83}	1.90936	148.75	O_{68}-Zn_{67}-O_{83}	
Zn_{71}	29.19	Zn_{71}-O_{68}	1.91142	137.68	O_{68}-Zn_{71}-O_{89}	
Zn_{84}	29.08	Zn_{84}-O_{89}	2.01804	110.64	O_{89}-Zn_{84}-O_{102}	
Zn_{91}	29.15	Zn_{91}-O_{83}	1.86818	132.48	O_{83}-Zn_{91}-O_{102}	
O_{35}	8.77	O_{35}-Zn_{34}	1.98172	119.78	Zn_{34}-O_{35}-Zn_{91}	D
O_{51}	8.88	O_{51}-Zn_{36}	2.15378	133.06	Zn_{36}-O_{51}-Zn_{53}	
O_{54}	8.75	O_{54}-Zn_{34}	1.85233	152.93	Zn_{34}-O_{54}-Zn_{53}	
O_{83}	8.76	O_{83}-Zn_{91}	1.86818	126.77	Zn_{91}-O_{83}-Zn_{101}	
O_{107}	8.89	O_{107}-Z_{n101}	1.94877	123.65	Zn_{36}-O_{107}-Zn_{101}	
Zn_{15}	29.21	Zn_{15}-O_{54}	1.82585	100.46	O_{51}-Zn_{15}-O_{54}	
Zn_{34}	29.21	Zn_{34}-O_{51}	2.01943	107.37	O_{35}-Zn_{34}-O_{54}	
Zn_{36}	29.18	Zn_{36}-O_{107}	2.18838	98.680	O_{51}-Zn_{36}-O_{107}	
Zn_{91}	29.15	Zn_{91}-O_{35}	2.03761	139.33	O_{35}-Zn_{91}-O_{83}	
Z_{n101}	29.14	Zn_{101}-O_{83}	2.08588	171.35	O_{83}-Zn_{101}-O_{107}	

The irregular ring-like formation of the final structure Fig. 4 has an eleven-sided structural asymmetric shape composed of Zn6 O5, with a Zn-Zn link protruding.

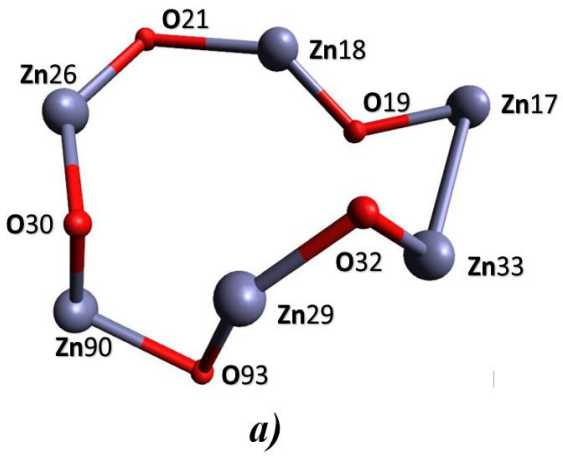

Fig. 8 The 11 atoms form a structure without a regular structural arrangement with two types of bonds prevailing between odd arrangements of structures, one oxygen with zinc and the other zinc with zinc

TABLE III: MULLIKEN POPULATION ANALYSIS, LENGTH AND ANGLE FOR FIG. 8

Mulliken population analysis		Distance		Angle *(°)*		
Atom	Charge	Bond	Length *(A)*	Angle *(°)*	Initial Atom - Vertex Atom Final Atom	
Zn_{17}	29.17	Zn_{17}-O_{19}	1.91015	54.906	O_{19}-Zn_{17}-Zn_{90}	A
Zn_{18}	29.14	Zn_{18}-O_{21}	2.20599	138.73	O_{19}-Zn_{18}-O_{21}	
Zn_{26}	29.10	Zn_{26}-O_{30}	1.93579	132.37	O_{21}-Zn_{26}-O_{30}	
Zn_{29}	29.19	Zn_{29}-O_{32}	1.87481	145.90	O_{32}-Zn_{29}-O_{93}	
Zn_{90}	29.26	Zn_{90}-O_{93}	2.17720	91.455	O_{30}-Zn_{90}.O_{33}	
O_{19}	8.81	O_{19}-Zn_{18}	1.81027	121.02	Zn_{17}-O_{19}-Zn_{18}	
O_{21}	8.94	O_{21}-Zn_{26}	1.92449	117.13	Zn_{18}-O_{21}-Zn_{26}	
O_{30}	8.80	O_{30}-Zn_{90}	1.92378	98.583	Zn_{26}-O_{30}-Zn_{90}	
O_{32}	8.83	O_{32}-Zn_{33}	1.93849	94.253	Zn_{29}-O_{32}-Zn_{33}	
O_{93}	8.72	Zn_{29}-O_{93}	1.95881	92.651	Zn_{29}-O_{93}-Zn_{90}	
Zn_{33}	29.21	Zn_{33}-Zn_{17}	2.77179	109.53	Zn_{17}-Zn_{33}-O_{32}	

IV. CONCLUSIONS

The experimental research in the synthesized nanomaterial structures reports various structural forms, which implies explaining whether there is a way to understand the formation of these structures. The results allow the following conclusions to be made: In the process of describing the reaction phenomena that occur in an interaction, a flat structure that simulates a monolayer was considered and placed as an initial starting point, a speed was applied that showed the formation of a new structure. The physical environment of oxygen atoms has a direction with a preference for the formation of pairs of Zn_{54} and O_{54}. In the analysis of the calculations for a two-layer model previously obtained by identifying aggregates of atoms where different molecular structures were obtained. The arrangements of atoms and the possible reaction mechanisms that occur when increasing the number of atoms with different tendencies depending on the direction is observed in the results that are assured there is generation of two-dimensional molecules that follow hexagons and are flat. In addition, continuing with the generation of a three-dimensional molecule it is affirmed that different structural forms occur at the end concluding that for a three-dimensional system the hexagons persist in the central part but the different structural forms of a nanomaterial are explained by the diversity of bonds that occur at the ends of this representative model of ZnO structures. The structural bonds with the number of odd atoms always have a zinc bond with zinc.

ACKNOWLEDGMENT

The authors thankfully acknowledge computer resources, technical advice, and support provided by LNS, a member of the CONACYT national laboratories with project No. 201801072-N, IPZ which would like to acknowledge their project TecNM. No. 6200.17-P. Cristian Eduardo thanks CONACYT for its scholarship No. CVU 897926.

REFERENCES

[1] E. G. Lewars andd P. Yates; *Computational Chemistry*, 1st ed. Kluwer Academic Publishers New York, Boston, Dordrecht, London, Moscow, 2004, pp 81- 157

[2] V Petukhov, J Stoemenos, J Rothman, A Bakin, A Waag; "Interpretation of transport measurements in ZnO-thin films" Applied Physics A,pp 1-8 June 2010

[3] J Tiekun, W Weimin, D Yanling, L Fei, F Zhengyi; *Controlling Growth of ZnO Nanostructures Via A Solution Route* Journal of Wuhan University of Technology-Mater. Sci. Ed. pp 249-253 Apr. 2009

[4] Y Zhang, F Zhu, J Zhang, L Xia, "Converting Layered Zinc Acetate Nanobelts to One-dimensional Structured ZnO Nanoparticle Aggregates and their Photocatalytic Activity Nanoscale" Res Lett (2008) 3: pp 201–204 June

[5] J.Y. Lao, J.Y. Huang, D.Z. Wang, Z.F. Ren, D. Steeves, B. Kimball, W. Porter; "*ZnO nanowalls*" Appl. Phys. A 78, 539–542 November 2003

[6] H Emrah, P Hiralal, D Kuo, B Parekh, G Amaratunga, and M Chhowalla; "Flexible organic photovoltaics from zinc oxide nanowires grown on transparent and conducting single walled carbon nanotube thin films" J. Mater. Chem., pp 1-9 November 2008

[7] H Zhou, G Fang, N Liu, X Zhao; "Ultraviolet photodetectors based on ZnO nanorods-seed layer effect and metal oxide modifying layer effect" Zhou et al. Nanoscale Research Letters pp 1-6 June 2011,

[8] H. C. Onga, A. X. E. Zhu; "Dependence of the excitonic transition energies and mosaicity on residual strain in ZnO thin films" Applied Physics Letters pp 941-943 FEBRUARY 2002

[9] W. Cheng, P. Wu, X. Zou, and T. Xiao; "*Study on synthesis and blue emission mechanism of ZnO tetrapodlike nanostructures"* American Institute of Physics, pp 1-4 September 2006.

[10] J. Hu and B. C. Pan; "The optical and vibrational properties of dominant defects in undoped ZnO: A first-principles study" American Institute of Physics, pp 1-5 April 2009.

[11] T. Okada, B.H. agung, Y Nakata; "*ZnO nano-rods synthesized by nano-particle-assisted pulsed-laser deposition*" Appl. Phys. A 79, pp 1417–1419 July (2004)

[12] C.Y. Tsay, K. S. Fan, C. Chen, J. M. Wu, C. M. Lei; "Effect of preheating process on crystallization and optical properties of sol-gel derived ZnO semiconductor thin films" J Electroceram October (2011) pp 23–27

[13] V.V. Zalamai, V.V. Ursaki, I.M Tiginyanu, A. Burlacu, E. V. Rusu C. Klingshirn, J. Fallert, J. Sartor, H. Kalt; "Impact of size upon lasing in ZnO microtetrapods" Appl Phys B: pp 215–222. (2010)

[14] A. Abdel Aal, S. A. Mahmoud, A. K. Aboul; "Sol–Gel and Thermally Evaporated Nanostructured Thin ZnO Films for Photocatalytic Degradation of Trichlorophenol," Nanoscale Res Lett pp 627–634 March 2009

[15] F. K. Farhan, Z. A. Ramadhan, and Widad A. A. Hussein; "Thermal Properties of UPE-PMMA Blend Reinforced by ZnO Nanoparticles" EJERS, European Journal of Engineering Research and Science Vol. 2, No. 7, pp 1-3 July 2017

[16] D. Pratap, "Singh Synthesis and Growth of ZnO Nanowires Science of Advanced Materials" Vol. 2, pp 245 - 272 May 2014.

[17] H. S. Bhatti, Atul Gupta, N. K.Verma, S. Kuma, "*Optical characterization of ZnO nanobelts"* J Mater Sci: Mater Electron pp 281–285 September, 2005

[18] Z. Fan, and J. G. Lu; "*Zinc Oxide Nanostructures: Synthesis and Properties"* Journal of Nanoscience and Nanotechnology Vol.5, pp 1–13, July 2015

[19] Z. Dai, A. Nurbawono, A. Zhang, M. Zhou, Y. P. Feng, G. W. Ho, and C. Zhang, "*C-doped ZnO nanowires: Electronic structures, magnetic properties, and a possible spintronic device"* The Journal of Chemical Physics 134, pp 1-5 March 2011

[20] A. D. Becke. "Density-functional exchange-energy approximation with correct asymptotic behavior" Phys. Rev A38, pp 3098 september 1988

[21] C lee, W Yang, and R. G. Part, "Development of the Colle-Salvetti correlation-energy formula into a functional of the electron density" Phys. Rev. B 37, pp 785 – January1988.